



**HAL**  
open science

## Metal stable isotopes in transplanted oysters as a new tool for monitoring anthropogenic metal bioaccumulation in marine environments: The case for copper

Daniel Ferreira Araujo, Joel Knoery, Nicolas Briant, Emmanuel Ponzevera, Tiphaine Chauvelon, Isabelle Auby, Santiago Yepez, Sandrine Bruzac, Teddy Sireau, Anne Pellouin-Grouhel, et al.

### ► To cite this version:

Daniel Ferreira Araujo, Joel Knoery, Nicolas Briant, Emmanuel Ponzevera, Tiphaine Chauvelon, et al.. Metal stable isotopes in transplanted oysters as a new tool for monitoring anthropogenic metal bioaccumulation in marine environments: The case for copper. *Environmental Pollution*, 2021, 290, 118012 (10p.). 10.1016/j.envpol.2021.118012 . hal-04203571

**HAL Id: hal-04203571**

**<https://hal.science/hal-04203571v1>**

Submitted on 22 Jul 2024

**HAL** is a multi-disciplinary open access archive for the deposit and dissemination of scientific research documents, whether they are published or not. The documents may come from teaching and research institutions in France or abroad, or from public or private research centers.

L'archive ouverte pluridisciplinaire **HAL**, est destinée au dépôt et à la diffusion de documents scientifiques de niveau recherche, publiés ou non, émanant des établissements d'enseignement et de recherche français ou étrangers, des laboratoires publics ou privés.



Distributed under a Creative Commons Attribution - NonCommercial 4.0 International License

## 1 **Metal stable isotopes in transplanted oysters as a new tool for monitoring anthropogenic** 2 **metal bioaccumulation in marine environments: the case for copper**

3 Daniel F. Araújo<sup>a\*</sup>, Joël Knoery<sup>a</sup>, Nicolas Briant<sup>a</sup>, Emmanuel Ponzevera<sup>b</sup>, Tiphaine Chouvelon<sup>a,c</sup>, Isabelle  
4 Auby<sup>d</sup>, Santiago Yepez<sup>e</sup>, Sandrine Bruzac<sup>a</sup>, Teddy Sireau<sup>a</sup>, Anne Pellouin-Grouhel<sup>f</sup>, Farida Akcha<sup>g</sup>

5 <sup>a</sup> Ifremer, Unité Biogéochimie et Écotoxicologie, Laboratoire de Biogéochimie des Contaminants Métalliques (BE/LBCM), Rue de  
6 l'Île d'Yeu, BP 21105, 44311 Nantes Cedex 03, France

7 <sup>b</sup> Ifremer, Unité Biogéochimie et Écotoxicologie (BE), Rue de l'Île d'Yeu, BP 21105, 44311 Nantes Cedex 03, France

8 <sup>c</sup> Observatoire Pelagis, UMS 3462 La Rochelle Université-CNRS, 5 allée de l'Océan, 17000 La Rochelle, France

9 <sup>d</sup> Ifremer, Unité Littoral, Laboratoire Environnement Ressources d'Arcachon (Littoral/LERAR), Quai du commandant Silhouette,  
10 33120 Arcachon, France

11 <sup>e</sup> Department of Forest Management and Environment, Faculty of Forestry, University of Concepcion, Calle Victoria, 500  
12 Concepción, Bio-Bio, Chile

13 <sup>f</sup> Ifremer, Unité Biogéochimie et Écotoxicologie (BE), Réseau d'Observation de la Contamination Chimique du littoral Rue de l'Île  
14 d'Yeu, BP 21105, 44311 Nantes Cedex 03, France

15 <sup>g</sup> Ifremer, Unité Biogéochimie et Écotoxicologie, Laboratoire d'Écotoxicologie (BE/LEX), Rue de l'Île d'Yeu, BP 21105, 44311  
16 Nantes Cedex 03, France

17 \*daniel.ferreira.araujo@ifremer.fr

### 18 **Abstract**

19 Metal release into the environment from anthropogenic activities may endanger ecosystems and  
20 human health. However, identifying and quantifying anthropogenic metal bioaccumulation in  
21 organisms remain a challenging task. In this work, we assess Cu isotopes in Pacific oysters (*C. gigas*)  
22 as a new tool for monitoring anthropogenic Cu bioaccumulation into marine environments. Arcachon  
23 Bay was taken as a natural laboratory due to its increasing contamination by Cu, and its relevance as a  
24 prominent shellfish production area. Here, we transplanted 18-month old oysters reared in an oceanic  
25 neighbor area into two Arcachon Bay mariculture sites under different exposure levels to continental  
26 Cu inputs. At the end of their 12-month long transplantation period, the oysters' Cu body burdens had  
27 increased, and was shifted toward more positive  $\delta^{65}\text{Cu}$  values. The gradient of Cu isotope  
28 compositions observed for oysters sampling stations was consistent with relative geographic distance  
29 and exposure intensities to unknown continental Cu sources. A binary isotope mixing model based on  
30 experimental data allowed to estimate the Cu continental fraction bioaccumulated in the transplanted  
31 oysters. The positive  $\delta^{65}\text{Cu}$  values and high bioaccumulated levels of Cu in transplanted oysters  
32 support that continental emissions are dominantly anthropogenic. However, identifying specific  
33 pollutant coastal source remained unelucidated mostly due to their broader and overlapping isotope  
34 signatures and potential post-depositional Cu isotope fractionation processes. Further investigations on  
35 isotope fractionation of Cu-based compounds in an aqueous medium may improve Cu source  
36 discrimination. Thus, using Cu as an example, this work combines for the first time a well-known  
37 caged bivalve approach with metal stable isotope techniques for monitoring and quantifying the  
38 bioaccumulation of anthropogenic metal into marine environments. Also, it states the main challenges  
39 to pinpoint specific coastal anthropogenic sources utilizing this approach and provides the perspectives  
40 for further studies to overcome them.

41 **Keywords:** metal bioaccumulation, non-traditional isotopes, bivalve mollusk, Arcachon Bay, MC-ICP-MS

## 42 **Introduction**

43 Metal pollution of aquatic environments inherently alters their chemical composition and poses  
44 health risks to ecosystems and humans (Fu et al., 2016; Gaetke et al., 2014; Reilly, 2004).  
45 Identifying the origins of metals that accumulate at any given site is a key step in developing  
46 successful emission control strategies and targeting contaminated sites for remediation (Barletta et  
47 al., 2019; de Souza Machado et al., 2016; Lu et al., 2018; Weiss et al., 2008). To this end, the  
48 study of the composition of metal stable isotopes in low-cost biomonitoring organisms may be a  
49 promising approach for identifying and quantifying anthropogenic inputs (Martín et al., 2018;  
50 Shiel et al., 2012; Smith et al., 2021, 2020). However, a prerequisite step is to examine the ability  
51 of this approach in discriminating between natural Cu (the geochemical background) and  
52 anthropized Cu, the latter being Cu released to the environment after its transformation within the  
53 anthroposphere.

54 In coastal and marine ecosystems, bivalve mollusks have been widely used in “Mussel  
55 Watch programs” for monitoring among other pollutants, marine trace metal (Krishnakumar et al.,  
56 2018; Lu et al., 2017; Zhou et al., 2008). Indeed, bivalves, such as oysters and mussels, combine  
57 several features that are advantageous for biomonitoring purposes: they are suspended matter  
58 filter-feeders, abundant, sessile, and relatively easy to collect and handle in the laboratory (Araújo  
59 et al., 2021a). Datasets of elemental levels in these organisms help obtain qualitative information  
60 about spatial and temporal trends on metal bioaccumulation, but physiological (e.g., body size,  
61 homeostasis) and environmental (e.g., salinity, primary production, phytoplankton assemblages)  
62 factors may be confounding, and prevent an accurate assessment of the influence of  
63 anthropogenic metal inputs in the environment (Briant et al., 2017; Cossa and Tabard, 2020; Lu et  
64 al., 2019, 2017; Pourmozaffar et al., 2019). In turn, metal stable isotopes and mixing models can  
65 potentially help track metals from their respective natural and/or anthropogenic origins, thus  
66 providing a more direct appreciation of anthropic influence (Araújo et al., 2021b). Indeed, isotope  
67 signatures of metals within the anthroposphere are associated with manufactured materials or their  
68 by-products. They result from their original sources (e.g., coal and ore deposits), modulated by  
69 their transformation processes, such as electroplating and smelting (Borrok et al., 2010; Brocza et  
70 al., 2019; Gonzalez and Weiss, 2015; Shiel et al., 2010; Sun, 2019; Tonhá et al., 2020; Zeng and  
71 Han, 2020; Zhong et al., 2021). Isotope signatures of metals circulating in the anthroposphere tend  
72 to differ from isotope compositions of metals occurring naturally in waters and sediments, which  
73 are modulated by weathering and biological activity (Araújo et al., 2019a; Babcsányi et al., 2014;  
74 Guinoiseau et al., 2017; Mulholland et al., 2015; Vance et al., 2016). In previous studies, Zn and  
75 Cd isotope records in wild bivalve’s soft tissues allowed to gauge and/or quantify anthropogenic  
76 inputs in marine environments (Araújo et al., 2021b; Shiel et al., 2013, 2012). These previous

77 works used bivalve samples provided by samples banks feed by Mussel Watch programs from  
78 France and United States, operating continuously since the 70s. Unfortunately, these national  
79 biomonitoring programs do not cover all marine sites, and they are inexistent in most countries.  
80 Transplanting bivalves from one ground to another is an alternative to circumvent the  
81 unavailability of bank samples. It has been commonly practiced to observed metal  
82 bioaccumulation trends in these organisms over determined periods (Geffard et al., 2002; Regoli  
83 and Orlando, 1994; Riget et al., 1997; Roméo et al., 2003; Séguin et al., 2016; Senez-Mello et al.,  
84 2020, 2020; Wallner-Kersanach et al., 2000). We are unaware of studies using “non-traditional”  
85 isotopes in transplanted organisms.

86 A first examination on the variations of Cu isotope abundances ( $^{65}\text{Cu}$  and  $^{63}\text{Cu}$ ) in soft  
87 tissues of wild bivalves (mussels and oysters) revealed the potential to obtain information related  
88 to Cu sources, bioaccumulation mechanisms, and physiological status (Araújo et al., 2021a). The  
89 latter study was conducted in a low-contaminated Atlantic site (Vilaine Bay) and integrated a 10-  
90 year biomonitoring period. It attributed the observed temporal isotope fractionation patterns of  
91 mussels to homeostatic regulation processes, involving changes in uptake and excretion rates with  
92 increasing Cu bioavailability. For oysters, Cu isotope compositions evolved linearly with Cu body  
93 burden, indicating a conservative isotope fractionation with Cu bioaccumulation over time.  
94 However, the use of this particular isotope bioaccumulation pattern observed in oysters to identify  
95 and quantify the biological incorporation of anthropogenic Cu remained untested. To continue this  
96 work, we conducted an *in-situ* experiment with transplanted and caged oysters in Atlantic oyster-  
97 rearing site recognized by its Cu-contamination history.

98 With up to 12000 tons/year, France is at present Europe’s top producer and consumer of  
99 Pacific oysters (*Crassostrea gigas*, Buestel et al., 2009), and environmental concerns with high Cu  
100 anthropogenic bioaccumulation in France’s farmed oysters dates back to the 1930s (Hinard, 1932).  
101 Arcachon Bay (AB) is the oldest French oyster-producing basin, where a continuous increase in  
102 Cu concentrations since 1982 is observed (Claisse and Alzieu, 1993; Fig. 1). Although Cu is an  
103 essential micronutrient for oysters, excessive environmental concentrations of this metal can  
104 damage endocrine systems and affect larval life stages, thus impacting ecological services  
105 provided by these organisms, and up to compromising mariculture production and food safety  
106 (Gamain et al., 2017; Mai et al., 2012; Sussarellu et al., 2018; Wang et al., 2011; Wijsman et al.,  
107 2019). The origin of the increased Cu observed in AB oysters was putatively attributed to the  
108 growing use by nautical activities of Cu-based antifouling paints after the ban of tributyltin (TBT),  
109 a biocide that had long entered in the composition of such paints (Claisse and Alzieu, 1993).  
110 Nevertheless, previous studies using Cu concentration data in sediment, water, and bivalves did  
111 not allow to pinpoint the origin of this increased Cu, and/or ascertain its bioaccumulation.

112 As a new approach for our study, bivalves originating from a coastal neighboring site were  
113 transplanted into AB and monitored for one year. Parameters included their elemental Cu levels,

114 Cu isotope compositions, and other biometric data, including shell length and weight of soft tissue  
115 parts. Transplanted, caged bivalves share their previous and identical environmental chemical  
116 exposure and life histories, and hence, they are advantageous to reduce possible isotope  
117 variabilities related to variations in environmental and biological factors (Benedicto et al., 2011;  
118 Caro et al., 2015; Ostrander, 1996; Senez-Mello et al., 2020). Since oysters were reared together  
119 and at the same site since their larval stage, we hypothesize that the differences in isotope  
120 fingerprints observed in transplanted oysters after a one-year exposure period reflect the different  
121 local Cu isotope signatures at the new site. In our study of the AB, observed isotope shifts in  
122 bivalves' soft tissues are attributable mainly to the bioaccumulation of Cu coming from coastal  
123 anthropogenic sources, rather than isotope changes affecting marine Cu. Thus, using Cu as an  
124 example, this work combines for the first time a well-known caged bivalve approach with metal  
125 stable isotope techniques for monitoring and quantifying the bioaccumulation of anthropogenic  
126 metals by these organisms into marine environments. Also, it states the main challenges to  
127 pinpoint specific coastal anthropogenic sources utilizing this approach and provides the  
128 perspectives for further studies to overcome them.

129

## 130 **Methods**

### 131 *Study area*

132 The Arcachon Bay (AB, 44°40'N, 01°10'W, Fig. 1) is a French macrotidal coastal lagoon (1 - 5 m  
133 tidal range, 156 km<sup>2</sup>) connected to the Atlantic Ocean by a 5 km long channel (Deborde et al.,  
134 2008). Surface seawater temperature ranges between 1 and 30 °C, and salinity is between 22 and  
135 32 psu, with a significant difference between western and eastern basins that are under the  
136 influence of oceanic and continental waters, respectively (Deborde et al., 2008). Shellfish farming  
137 activities are characteristic of the local culture and economy, which started at the end of the 19th  
138 century. The perimeter of AB is entirely lined by suburban centers and associated marinas (Fig. 1).  
139 The port of Arcachon is one main leisure port of of the French Atlantic coast, accounting about  
140 12,000 registered boats, which 95% of pleasure crafts, and the rest are used for fishing, oyster  
141 farming and maritime transport (Le Berre et al., 2010). A census performed in the early 2000's  
142 showed that most of these embarkations now use annually about 4,3m<sup>3</sup> of copper-based  
143 antifouling paints since TBT paints were banned (Auby and Maurer, 2004).. Thus, the sheer  
144 intensity of leisure boating activities interacts strongly with AB's natural environment and its  
145 professional users (Le Berre et al., 2010). The inner basin is affected by a major source of fresh  
146 water by the Leyre River, and other small rivers that flow into the lagoon (Rimmelin et al., 1998).  
147 The farm activities in the Leyre river watershed (Fig. 1) are a source of pesticides in the AB  
148 (Fauvelle et al., 2018).

149

### 150 *Oyster transplantation experiment and wild oyster collection*

151 One thousand 18-month-old *C. gigas* oysters were used for the transplantation experiment. They  
152 originated from the “Arguin Banc” site in the open Bay of Biscay, and presumably fully under  
153 oceanic influence (Fig. 1), and were transplanted in AB where they were held in polyethylene  
154 mesh bags used as cages. This pool of oysters was sub-divided into two 500-organism batches  
155 that were transplanted on 30th March 2017 (beginning of the study, T<sub>0</sub>) at the sites of “Comprian”  
156 (inner AB) and “Grand Banc” (outer AB, Fig. 1). At each time point, ca. 80 individual oysters  
157 were collected from each site after 3-, 6-, and 12-month exposure periods.

158 After collection, bivalves were depurated in laboratory tanks during 24 h, using filtered  
159 local seawater. Then, 30 specimens were taken for biometric measurements, including shell length  
160 and weight, total body weight, and the weight of their lyophilized soft tissues (namely dry tissue),  
161 to quantify their growth using a body condition index: (weights of dry tissue / (total body tissue –  
162 shell) \* 1000; (Lawrence and Scott, 1982). Depending on the weight of the organisms, soft parts  
163 of between 20 and 50 individuals were pooled, homogenized, and dried for the metal analyses  
164 presented here. The average bioaccumulated Cu body burden ( $\mu\text{g Cu}$  per individual bivalve) in the  
165 soft tissues of each pool was estimated by multiplying Cu concentrations of the pool by the  
166 corresponding mean dry weight of the soft tissues. This is meant to accommodate differences in  
167 growth rates and neutralize biodilution.

168 In AB, there are three oyster sampling stations from the French marine chemical  
169 contamination biomonitoring network ROCCH. These stations, which include the Comprian site,  
170 have been using indigenous oysters to monitor marine contaminants, including TBT and Cu, since  
171 1980 (<https://wwz.ifremer.fr/surval/>). For an example, Fig. 1 shows a time series of Cu and TBT  
172 levels in oysters from Comprian. For our study, an additional sample made of lyophilized soft  
173 tissues of ca. ten indigenous oysters from Comprian and collected in the winter of 2019 and  
174 prepared identically to the transplanted oysters within the biomonitoring framework of the  
175 ROCCH.

176

### 177 *Sample preparation and analyses*

178 Bivalve sample digestion and chemical analysis have already been detailed in previous  
179 publications (Araújo et al., 2019,a,b; 2021a,b). Briefly, aliquots of freeze-dried bivalve tissues  
180 (~200 mg) were digested in closed vessels by a concentrated nitric acid solution and using  
181 microwave energy. Copper elemental analyses were performed by quadrupole inductively coupled  
182 plasma mass spectrometry (ICP-MS). For isotope analyses, aliquots of digested samples  
183 containing 500 ng of Cu were purified using an AG-MP1 resin, and Cu isotope abundances  
184 determined by multicollector ICP-MS (Neptune, Thermo Scientific) at the Pôle Spectrométrie  
185 Océan (PSO) laboratory (Ifremer, France). Reference materials (RMs) of other animal tissues  
186 (oyster SRM 1566b-NIST®; protein fish DORM-4, NRC-CNRC®) and procedural blanks were

187 included in each sample batch for analytical control. All sample preparation procedures were  
188 carried out with ultrapure water and high-purity acid blends.

189 Isotope analyses samples were dissolved in diluted acid nitric (2% v/v) and analyzed at  
190 concentrations around 250 ng g<sup>-1</sup>. A Stable Introduction System (SIS: cyclonic spray chamber and  
191 PFA nebulizer at 50 μL min<sup>-1</sup>, ESI) was used to introduce samples into spectrometer. The raw Cu  
192 isotope ratios were corrected for mass bias using the standard bracketing technique and the final  
193 Cu isotope compositions expressed using the conventional δ-notation relative to the isotope  
194 certified reference material NIST SRM-976 (Eq. 1):

$$195 \quad \delta^{65}\text{Cu}_{\text{SRM-976}}(\text{‰}) = \left( \frac{R\left(\frac{^{65}\text{Cu}}{^{63}\text{Cu}}\right)_{\text{sample}}}{R\left(\frac{^{65}\text{Cu}}{^{63}\text{Cu}}\right)_{\text{SRM-976}}} - 1 \right) \times 1000 \quad (\text{Eq. 1})$$

196  
197 For unknown samples and RMs, δ<sup>65</sup>Cu<sub>SRM-976</sub> values represent the average and the two-standard  
198 deviation (2s) of two or three individual measurements performed during a single analytical  
199 session. The precision average obtained for individual samples and RMs was better than ±0.05‰.  
200 The obtained δ<sup>65</sup>Cu<sub>SRM-976</sub> value for the RM fish protein DORM-4 (+0.55 ± 0.02‰, Table 1) fell  
201 in the same range of values published for this material (+0.52 ± 0.08‰, Sullivan et al., 2020;  
202 +0.48 ± 0.06‰, Sauzéat et al., 2021). The δ<sup>65</sup>Cu<sub>SRM-976</sub> value obtained for three full replicates of  
203 the oyster tissue SRM 1566b of +0.25 ± 0.03‰ is in line with the long-term reproducibility for  
204 this RM (+0.22 ± 0.03‰, 2s, n = 8, Araújo et al., 2021) at PSO laboratory.

205

## 206 **Results and discussion**

207

### 208 *Evolution of bioaccumulated Cu and its isotope composition in transplanted oysters*

209 The dataset is presented in Table 1, and all biometric data are included in the Supplementary  
210 Material (Table 1S). The biometric data indicate a faster and higher body growth of oysters in  
211 Grand Banc (outer AB) compared to those in Comprian (inner AB, Table 1S). Hence, to cancel  
212 out effects of biodilution in Cu concentrations and to be able to compare Cu bioaccumulation  
213 despite growth rate differences between these sites, we computed the oysters' Cu body burden (μg  
214 Cu/per individual, Table 1) rather than Cu concentrations.

215 Oysters transplanted in Comprian and Grand Banc sites shared temporal patterns of Cu  
216 concentration, body burden, and isotope compositions, i.e., a significant increase in the  
217 concentration of bioaccumulated Cu accompanied by a shift toward more positive δ<sup>65</sup>Cu values  
218 (Fig. 2, Table 1). In Comprian, over the one-year exposure period, mean oyster Cu body burdens  
219 increased continuously from 44 to 189 μg (four-fold increase), while δ<sup>65</sup>Cu values shifted from  
220 +0.35 to +0.60‰. The latter is remarkably close to indigenous oysters from Comprian harvested  
221 in winter 2019 (+0.59‰, Fig. 2). In Grand Banc, the Cu body burden levels are lower than in

222 Comprian at the 3-month and 6-month time steps, but reach a very similar 188  $\mu\text{g}/\text{per individual}$   
223 (Fig. 2a) at the end of the exposure period. In turn, the Cu isotope composition does not evolve  
224 monotonously, with an initial shift to lower  $\delta^{65}\text{Cu}$  values at the first-time step followed by an  
225 increase and stabilization near 0.4‰ (Fig. 2b). Despite comparable Cu body burdens at the 2 AB  
226 sites reached at the end of the transplantation experiment, the oysters' final isotope compositions  
227 differ by 0.17‰ (Fig. 3a). It is also notable that the largest isotope shift occurs at Comprian, about  
228 0.25‰.

229 The temporal changes from initial  $\delta^{65}\text{Cu}$  values in oyster soft parts, and the increase of Cu  
230 body burden and concentration suggest that bioaccumulated Cu in AB has a distinct origin from  
231 that offshore, at the Arguin Banc site (Fig. 3a). In line with our initial hypothesis, the simultaneous  
232 and linear increases of elemental body burden and isotope compositions shows that there exists a  
233 pool of bioavailable Cu inside the AB which is distinct from the offshore marine environment.  
234 The faster Cu bioaccumulation and larger magnitudes of isotope variation in oysters from  
235 Comprian (inner AB) suggest that this area is under greater exposure to continental Cu emissions.  
236 (Fig. 3a). This is possibly due to its geographic proximity to agriculture and urban sources from  
237 the Leyre watershed and/or the influence from nautical releases (antifouling paints) from the inner  
238 bay. In contrast, the more restricted isotope variations and lower Cu bioaccumulation rates in  
239 Grand Banc (outer AB) are consistent with the more oceanic character of this site, which also  
240 captures an attenuated and temporally-delayed continental Cu signal. The observed shift to lower  
241  $\delta^{65}\text{Cu}$  values in the first three months of the transplantation experiment (GB-T1 sample in outer  
242 AB) is attributed to off-shore seawater during the summer (low river flow). Indeed, estuarine  
243 waters from the neighboring Gironde estuary (Atlantic French coast) with low anthropogenic Cu  
244 displayed enrichments in light isotope about  $+0.12 \pm 0.08\text{‰}$  (1s, n= 8, Petit et al., 2013), which  
245 supports this proposition. Indeed, as will see in the further discussion, the estimated end-member  
246 of marine bioaccumulated Cu pool for oysters matches well with a low  $\delta^{65}\text{Cu}$  value for oceanic  
247 waters.

248

249 *Inferring a Cu binary source model to apportion the continental and natural Cu fractions*  
250 *bioaccumulated in oysters*

251 The gradient of Cu isotope compositions observed for oyster soft parts at Comprian and Grand  
252 Banc sampling stations was consistent with exposure intensities to a continental Cu source.  
253 Plotting  $\delta^{65}\text{Cu}$  values against its reciprocal concentration ( $1/[\text{Cu}]$ ) is a useful approach to identify  
254 source mixing processes (El Azzi et al., 2013; Křibek et al., 2018; Mihaljevič et al., 2019). The  
255 good fit of all oyster samples (indigenous and transplanted) on a straight line ( $R^2 = 0.93$ ,  $p < 0.05$ )  
256 indicate that bioaccumulated Cu and associated  $\delta^{65}\text{Cu}$  values can be described in terms of a simple  
257 binary mixing source model involving two end-members, defined here as representing the  
258 continental and marine bioavailable Cu pools in oysters, respectively (Fig. 3b). The “mixture line”



259 obtained by regression analysis allow to estimate the values of these two end-members, which in  
260 turn can then be used to quantify the continental Cu fraction bioaccumulated in oysters. As noted,  
261 these end-members represent bioaccumulated pools of Cu, rather than actual Cu sources to this  
262 environment. Since they are based on the oyster dataset, they already include any potential  
263 biological isotope fractionation induced by oyster Cu bioaccumulation. Therefore, they can be  
264 used to quantify the continental Cu fraction bioaccumulated in oysters' soft tissues irrespectively  
265 of any biological fractionation. The implications in their use for source identification are discussed  
266 in next section.

267 By substituting a global natural concentration baseline of Cu in oysters ( $\sim 34 \text{ mg kg}^{-1}$ , Lu et  
268 al., 2019) in the linear regression equation, we obtain  $+0.02\text{‰}$  for an isotopic end-member  
269 representing the natural marine Cu bioaccumulated pool at our study site. Interestingly, this value  
270 is close to some relatively unpolluted estuarine water samples from the neighboring Gironde  
271 estuary (Atlantic French coast,  $+0.12 \pm 0.08\text{‰}$ , 1s,  $n = 8$ , Petit et al., 2013). For the other end-  
272 member, we use the highest Cu concentration reported in oysters from the French Mussel Watch  
273 program (of approximately  $2,500 \text{ mg.kg}^{-1}$ ) to obtain a value about  $+0.65\text{‰}$  for the continental  
274 bioaccumulated Cu end-member (Fig. 3b). This extrapolation towards low and elevated Cu  
275 concentrations is consistent with the exceptional capacity of oysters to bioaccumulate high loads  
276 of Cu, as high as 4 % d.w. of whole-body tissue (Wang et al., 2011). The standard error of the  
277 regression analysis (S), which represents the average distance that the observed values fall from  
278 the regression curve, is about  $\pm 0.05 \text{‰}$  and is considered the uncertainty associated with the  
279 estimation of the two end-member values.

280 The calculated  $\delta^{65}\text{Cu}$  end-member values of  $+0.65 \text{‰}$  and  $+0.02 \text{‰}$  enable the use of a  
281 simple binary mixing model to quantify respectively the relative fractions of continental and  
282 marine Cu fractions bioaccumulated in their soft tissues during the time-course of the  
283 transplantation:

284

$$285 \quad \text{Cu}_{\text{continental}}(\%) = \left( \frac{\delta^{65}\text{Cu}_{\text{sample}} - \delta^{65}\text{Cu}_{\text{marine}}}{\delta^{65}\text{Cu}_{\text{continental}} - \delta^{65}\text{Cu}_{\text{marine}}} \right) * 100 \text{ (Eq. 2)}$$

286

287 where  $\delta^{65}\text{Cu}_{\text{sample}}$ ,  $\delta^{65}\text{Cu}_{\text{natural}}$ , and  $\delta^{65}\text{Cu}_{\text{anthropogenic}}$  stand for the  $\delta^{65}\text{Cu}$  values obtained for the  
288 sample of interest, and the estimated values for natural and anthropogenic Cu end-members,  
289 respectively. The computed values are included in Table 1. Uncertainty values were computed by  
290 error propagation in Equation 2 using analytical uncertainties of oyster samples (Table 1) and  
291 estimate uncertainties of end-members ( $\pm 0.05\text{‰}$ ) were below 1% for transplanted oysters.

292 The Cu of continental origin bioaccumulated in oysters before transplantation amounts to  
293 52 %, revealing the transport of continental emissions to the marine environments beyond AB. In  
294 the transplanted oysters from Comprian, this percentage climbs to 92%, matching closely this of

295 indigenous oysters (90%). Even if oysters from Grand Banc display similar Cu bioaccumulation  
296 loads (Table 1), the continental Cu fraction is significant, with a contribution of 65 % to the Cu  
297 body burden. As a consistency check, we use the concentration presented in Fig. 1. It shows that  
298 the Cu concentrations in contemporary oysters have nearly quadrupled over the last 40 years,  
299 indicating the “new” Cu incoming AB unlikely to derive from natural sources. It is reassuring that  
300 the  $\frac{3}{4}$  of continental Cu in present-day oysters estimated from the time series is close to the  
301 isotopically-calculated fraction. Most anthropic sources reported in the literature, including  
302 antifouling and urban sources, display more positive Cu isotope composition averages than the  
303 Upper Continental Crust, which isotope range is about 0‰ (Fig. 4). Therefore, it is plausible that  
304 the bioaccumulation of Cu emitted from coastal anthropogenic sources shifts oyster’s isotope  
305 compositions to positive values, such as observed in our study. Thus, we consider continental Cu  
306 emissions in AB dominantly anthropogenic. The following section discusses the potential use of  
307 oyster’s isotope signatures to pinpoint anthropogenic Cu sources.

308

### 309 *A critical assessment of using recorded Cu isotope signals in oysters for source identification*

310 Using oyster isotope signatures for source identification requires verifying if biological uptake and  
311 biogeochemical processes in sediment-water interface can overprint original isotope signatures of  
312 sources. Here, we assess the potential effect of these factors on Cu isotope signals recorded in  
313 oysters.

314 Oysters can accumulate Cu (and Zn) at high concentrations without serious toxic effects,  
315 due to great capacity for detoxifying excess Cu and Zn by making these metals under inert and  
316 non-toxic forms. Presumably, this mechanism compensates for their lack of significant cellular Zn  
317 and Cu excretion (Kunene et al., 2021; Rainbow, 2018; Wang et al., 2018, 2011). Indeed, the  
318 “half-lives” calculated for Cu and Zn excretion from the same *C. gigas* species from the  
319 neighboring Gironde estuary Atlantic Coast, are about 1,500 and 3,000 days, respectively  
320 (Geffard et al., 2002). These durations are very long compared to the life-spans of our oysters, and  
321 are consistent with the limited elimination of these elements into inert, intracellular, metal-rich  
322 granules (Geffard et al., 2002; Wang et al., 2018). Thus, these very low excretion rates of Cu and  
323 Zn in oysters likely to not affect isotope budget of whole soft tissues, which makes these  
324 organisms “integrative isotope recorders” of the source contributions in the bioaccumulated Cu  
325 and Zn from their surrounding environment. While this has already been shown for Zn isotopes in  
326 oysters in aquarium-based experiments (Ma et al., 2019), it is still to be rigorously confirmed for  
327 Cu. However, based on the similarity of bioaccumulation mechanisms for these both  
328 micronutrient elements (Kunene et al., 2021; Tan et al., 2015, Weng et al. 2018), and the data  
329 presented above, we can speculate that it is also true for Cu.

330 Thus, we attribute the greatest difficulty to pinpoint anthropogenic Cu not to biological  
331 fractionation processes, but rather to the gaps in ours constrain about Cu isotope fractionation in

332 anthroposphere (Tonhá et al., 2020; Viers et al., 2018; Yin et al., 2018). Anthropogenic isotope  
333 signatures latter derive mainly from mineral deposits of this element, which present the most  
334 extensive range among the natural compartments ( $-16.5$  to  $+10$  ‰, Klein and Rose, 2020; Mathu  
335 and Wang, 2019; Moynier et al., 2017; Wang et al., 2017). Consequently, anthropogenic sources  
336 also display a wide isotope variability that can overlap each other, hampering the discrimination of  
337 individual Cu anthropogenic sources (Fig. 4). This drawback becomes more critical in complex  
338 coastal environments where several anthropogenic metal sources normally coexist.

339 It is worthy also to argue that the direct comparison of Cu isotope compositions between  
340 distinct, but connected marine biogeochemical reservoirs (e.g., sediment, water, biota) and  
341 anthropogenic materials is also fraught with uncertainties due to potential isotope fractionation  
342 that may occur during release and transfer between these environmental compartments before  
343 bioaccumulation. As an example, in Cu-polluted soils by Cu-based fungicide, soil particle  
344 leaching and surface runoff exhibit a shift up to  $0.40$  ‰ in comparison to the particulate phase  
345 source (Babcsányi et al., 2016; Blotevogel et al., 2018; El Azzi et al., 2013). In marinas and  
346 harbors, sediments that have been Cu-contaminated by antifouling paints show isotope signatures  
347 slightly lighter than the source anti-fouling paints themselves, but significantly different from the  
348 natural background (Briant, 2014). This suggests a preferential release of heavy isotopes from  
349 these compounds when solubilized in seawater, or the occurrence of an unaccounted fractionation  
350 process between the paint chip and its host sediment. Similar modifications on source isotope  
351 signatures induced by changes in the metal speciation have also been observed for Zn, Hg, and Cd  
352 isotope systems in sites with industrial and metallurgical contamination legacies or in laboratory  
353 involving photochemical reactions of Ag-nanoparticles (Tonhá et al., 2020; Brocza et al., 2019; Li  
354 et al., 2021; Shiel et al., 2010; Zhong et al., 2020).

355 It is noted that anthropogenic fingerprints in natural sample archives like sediments,  
356 exceed in amplitude the isotope range from the natural Cu baseline. The latter normally centered  
357 around  $0$  ‰ (Fig. 4). This isotope pattern is illustrated when comparing sediment from almost  
358 pristine to highly contaminated sites, like those of the Loire estuary, Port Camargue, and Toulon  
359 Bay (Fig. 4). The latter is characterized by lighter isotope signatures related to warfare and  
360 shipbuilding contamination legacies that ranges from  $-0.79$  to  $+0.34$  ‰ (Araújo et al., 2019a). In  
361 contrast, Port Camargue sediments range from  $-0.13$  to  $+0.44$  ‰ (Briant, 2014), tending in overall,  
362 to more positive values related to Cu-based antifouling paints. In turn, the relatively  
363 uncontaminated Loire estuary sediments have a narrower isotope range, with  $\delta^{65}\text{Cu}$  values  
364 between  $-0.24$  and  $+0.09$  ‰, with an average of  $-0.04 \pm 0.18$  ‰ (2s, n = 31). This average value is  
365 close to that of UCC ( $\sim 0$  ‰) and likely reflect the variability of its natural sources, such as  
366 weathered particles derived from soils and rocks of the Loire river watershed (Araújo et al.,  
367 2019b).

368           These studies and ours demonstrate that Cu isotopes can be useful to discriminate  
369 anthropogenic and natural sources in despite of possible isotope modifications of anthropogenic  
370 metals after their release into the environment. While identifying specific coastal sources remain  
371 a challenge task because these post-depositional isotope changes, they still carry isotope signals  
372 that can be traced and apportioned in particulate and dissolved phases, and ultimately, into the  
373 organisms.

374

### 375 *Conclusions*

376 This study confirmed, for the first time, the applicability of a “non-traditional” metal stable  
377 isotope system in transplanted oysters to monitor metal bioaccumulation. Our findings  
378 demonstrate that Cu isotopes can constrain the continental Cu fraction bioaccumulated in oysters  
379 and infer its natural or anthropogenic origin. The present methodology of transplanting oysters  
380 into an environmental contamination gradient can be extended to other metal isotope systems and  
381 then yield an apportionment of anthropogenic contributions to the metal body burden of these  
382 organisms. Furthermore, it does not hinge on the availability of sample banks of costly  
383 environmental monitoring networks operating for long time series.

384           Unfortunately, source pinpointing remains elusive and further studies are sorely needed.  
385 Indeed, the biogeochemical reactions of anthropogenic metal-based substances released into  
386 aquatic environments may potentially induce fractionation of metal isotopes between particulate  
387 and dissolved phases. This results mainly from changes in the metal atom’s coordination, strength  
388 of bonds, ligand complexation (inner-sphere vs. outer-sphere formations), and adsorbent features  
389 on the water column (Balistrieri et al., 2008; Dong and Wasylenki, 2016; Ducher et al., 2016;  
390 Guinoiseau et al., 2016; Li et al., 2015; Lu et al., 2016; Moynier et al., 2017). Thus, further  
391 laboratory and field experiments are required to observe and model how anthropogenic metals  
392 from a range of compounds known to contaminate marine environment yield different isotope  
393 signals in particulate and dissolved phases. For Cu isotopes, in the context of marine pollution,  
394 Cu-based anti-fouling paints are an obvious first experimental target.

395           Nevertheless, the combined use of several isotope systems, like Zn, Cd, Ag, and Pb in the  
396 so-called “multi-isotope approaches”, which have been successfully applied to individual pollutant  
397 tracking (Araújo et al., 2021c; Li et al., 2019; Shiel et al., 2012), could enhance their power of  
398 discrimination for different metal pollutant sources. This multi-isotope approach is timely for  
399 environmental forensic applications addressing pollution source identification in marine  
400 environments, since concentrations of trace metals, notably Cu, Zn, and Ag, are on the rise in  
401 urbanized marine coasts (Barletta et al., 2019; Zalasiewicz, 2018), or still present in mobile and  
402 bioavailable forms in legacy inventories (Araújo et al., 2019a; Briant et al., 2013; Caplat et al.,  
403 2005; Dang et al., 2015b, 2015a; Resongles et al., 2014; Tonhá et al., 2020).

404

## 405 Acknowledgments

406 This study has been carried out with financial support from the French National Research Agency  
407 (ANR) in the frame of the Investments for the Future Programme, within the Cluster of Excellence  
408 COTE (ANR-10-LABX-45). The authors thank to Dr. Runsheng Yin and the other anonymous  
409 reviewers for comments and corrections in the original version of this manuscript.

410

## 411 References

- 412 Araújo, D.F., Ponzevera, E., Briant, N., Knoery, J., Bruzac, S., Sireau, T., Brach-Papa, C., 2019a. Copper,  
413 zinc and lead isotope signatures of sediments from a mediterranean coastal bay impacted by naval  
414 activities and urban sources. *Applied Geochemistry* 111, 104440.  
415 <https://doi.org/10.1016/j.apgeochem.2019.104440>
- 416 Araújo, D.F., Ponzevera, E., Briant, N., Knoery, J., Bruzac, S., Sireau, T., Brach-Papa, C., 2019b. Copper,  
417 zinc and lead isotope signatures of sediments from a mediterranean coastal bay impacted by naval  
418 activities and urban sources. *Applied Geochemistry* 111, 104440.  
419 <https://doi.org/10.1016/j.apgeochem.2019.104440>
- 420 Araújo, D.F., Ponzevera, E., Briant, N., Knoery, J., Bruzac, S., Sireau, T., Pellouin-Grouhel, A., Brach-  
421 Papa, C., 2021a. Differences in Copper Isotope Fractionation Between Mussels (Regulators) and  
422 Oysters (Hyperaccumulators): Insights from a Ten-Year Biomonitoring Study. *Environ. Sci.*  
423 *Technol.* 55, 324–330. <https://doi.org/10.1021/acs.est.0c04691>
- 424 Araújo, D.F., Ponzevera, E., Briant, N., Knoery, J., Sireau, T., Mojtahid, M., Metzger, E., Brach-Papa, C.,  
425 2019c. Assessment of the metal contamination evolution in the Loire estuary using Cu and Zn  
426 stable isotopes and geochemical data in sediments. *Marine Pollution Bulletin* 143, 12–23.  
427 <https://doi.org/10.1016/j.marpolbul.2019.04.034>
- 428 Araújo, D.F., Ponzevera, E., Weiss, D.J., Knoery, J., Briant, N., Yopez, S., Bruzac, S., Sireau, T., Brach-  
429 Papa, C., 2021b. Application of Zn Isotope Compositions in Oysters to Monitor and Quantify  
430 Anthropogenic Zn Bioaccumulation in Marine Environments over Four Decades: A “Mussel  
431 Watch Program” Upgrade. *ACS EST Water* 1, 1035–1046.  
432 <https://doi.org/10.1021/acsestwater.1c00010>
- 433 Araújo, D.F., Ponzevera, E., Weiss, D.J., Knoery, J., Briant, N., Yopez, S., Bruzac, S., Sireau, T., Brach-  
434 Papa, C., 2021c. Application of Zn Isotope Compositions in Oysters to Monitor and Quantify  
435 Anthropogenic Zn Bioaccumulation in Marine Environments over Four Decades: A “Mussel  
436 Watch Program” Upgrade. *ACS EST Water*. <https://doi.org/10.1021/acsestwater.1c00010>
- 437 Auby, I., Maurer, Danièle, 2004. Etude de la reproduction de l’huître creuse dans le Bassin d’Arcachon.
- 438 Babcsányi, I., Chabaux, F., Granet, M., Meite, F., Payraudeau, S., Duplay, J., Imfeld, G., 2016. Copper in  
439 soil fractions and runoff in a vineyard catchment: Insights from copper stable isotopes. *Science of*  
440 *The Total Environment* 557–558, 154–162. <https://doi.org/10.1016/j.scitotenv.2016.03.037>
- 441 Babcsányi, I., Imfeld, G., Granet, M., Chabaux, F., 2014. Copper Stable Isotopes To Trace Copper  
442 Behavior in Wetland Systems. *Environ. Sci. Technol.* 48, 5520–5529.  
443 <https://doi.org/10.1021/es405688v>
- 444 Balistrieri, L.S., Borrok, D.M., Wanty, R.B., Ridley, W.I., 2008. Fractionation of Cu and Zn isotopes  
445 during adsorption onto amorphous Fe(III) oxyhydroxide: Experimental mixing of acid rock  
446 drainage and ambient river water. *Geochimica et Cosmochimica Acta* 72, 311–328.  
447 <https://doi.org/10.1016/j.gca.2007.11.013>
- 448 Barletta, M., Lima, A.R.A., Costa, M.F., 2019. Distribution, sources and consequences of nutrients,  
449 persistent organic pollutants, metals and microplastics in South American estuaries. *Science of The*  
450 *Total Environment* 651, 1199–1218. <https://doi.org/10.1016/j.scitotenv.2018.09.276>
- 451 Benedicto, J., Andral, B., Martínez-Gómez, C., Guitart, C., Deudero, S., Cento, A., Scarpato, A., Caixach,  
452 J., Benbrahim, S., Chouba, L., Boulahdid, M., Galgani, F., 2011. A large scale survey of trace  
453 metal levels in coastal waters of the Western Mediterranean basin using caged mussels (*Mytilus*  
454 *galloprovincialis*). *J. Environ. Monit.* 13, 1495–1505. <https://doi.org/10.1039/C0EM00725K>
- 455 Blotevogel, S., Oliva, P., Sobanska, S., Viers, J., Vezin, H., Audry, S., Prunier, J., Darrozes, J., Orgogozo,  
456 L., Courjault-Radé, P., Schreck, E., 2018. The fate of Cu pesticides in vineyard soils: A case study  
457 using  $\delta^{65}\text{Cu}$  isotope ratios and EPR analysis. *Chemical Geology* 477, 35–46.  
458 <https://doi.org/10.1016/j.chemgeo.2017.11.032>

- 459 Borrok, D.M., Gieré, R., Ren, M., Landa, E.R., 2010. Zinc Isotopic Composition of Particulate Matter  
460 Generated during the Combustion of Coal and Coal + Tire-Derived Fuels. *Environ. Sci. Technol.*  
461 44, 9219–9224. <https://doi.org/10.1021/es102439g>
- 462 Briant, N., 2014. Devenir et biodisponibilité du Cu, Zn et TBT dans un environnement portuaire fortement  
463 contaminé : la marina de Port Camargue. Montpellier 2.
- 464 Briant, N., Bancon-Montigny, C., Elbaz-Poulichet, F., Freydie, R., Delpoux, S., Cossa, D., 2013. Trace  
465 elements in the sediments of a large Mediterranean marina (Port Camargue, France): Levels and  
466 contamination history. *Marine Pollution Bulletin* 73, 78–85.  
467 <https://doi.org/10.1016/j.marpolbul.2013.05.038>
- 468 Briant, N., Chouvelon, T., Martinez, L., Brach-Papa, C., Chiffolleau, J., Savoye, N., Sonke, J., Knoery, J.,  
469 2017. Spatial and temporal distribution of mercury and methylmercury in bivalves from the French  
470 coastline. *Marine Pollution Bulletin* 114, 1096–1102.  
471 <https://doi.org/10.1016/j.marpolbul.2016.10.018>
- 472 Brocza, F.M., Biester, H., Richard, J.-H., Kraemer, S.M., Wiederhold, J.G., 2019. Mercury Isotope  
473 Fractionation in the Subsurface of a Hg(II) Chloride-Contaminated Industrial Legacy Site. *Environ.*  
474 *Sci. Technol.* 53, 7296–7305. <https://doi.org/10.1021/acs.est.9b00619>
- 475 Buestel, D., Ropert, M., Prou, J., Gouilletquer, P., 2009. History, Status, and Future of Oyster Culture in  
476 France. *Journal of Shellfish Research* 28, 813–820. <https://doi.org/10.2983/035.028.0410>
- 477 Caplat, C., Texier, H., Barillier, D., Lelievre, C., 2005. Heavy metals mobility in harbour contaminated  
478 sediments: The case of Port-en-Bessin. *Marine Pollution Bulletin* 50, 504–511.  
479 <https://doi.org/10.1016/j.marpolbul.2004.08.004>
- 480 Caro, A., Chereau, G., Briant, N., Roques, C., Freydie, R., Delpoux, S., Escalas, A., Elbaz-Poulichet, F.,  
481 2015. Contrasted responses of *Ruditapes decussatus* (filter and deposit feeding) and *Loripes lacteus*  
482 (symbiotic) exposed to polymetallic contamination (Port-Camargue, France). *Science of The Total*  
483 *Environment* 505, 526–534. <https://doi.org/10.1016/j.scitotenv.2014.10.001>
- 484 Claisse, D., Alzieu, C., 1993. Copper contamination as a result of antifouling paint regulations? *Marine*  
485 *Pollution Bulletin* 26, 395–397. [https://doi.org/10.1016/0025-326X\(93\)90188-P](https://doi.org/10.1016/0025-326X(93)90188-P)
- 486 Cossa, D., Tabard, A.-M., 2020. Mercury in Marine Mussels from the St. Lawrence Estuary and Gulf  
487 (Canada): A Mussel Watch Survey Revisited after 40 Years. *Applied Sciences* 10, 7556.  
488 <https://doi.org/10.3390/app10217556>
- 489 Dang, D.H., Lenoble, V., Durrieu, G., Omanović, D., Mullot, J.-U., Mounier, S., Garnier, C., 2015a.  
490 Seasonal variations of coastal sedimentary trace metals cycling: Insight on the effect of manganese  
491 and iron (oxy)hydroxides, sulphide and organic matter. *Marine Pollution Bulletin* 92, 113–124.  
492 <https://doi.org/10.1016/j.marpolbul.2014.12.048>
- 493 Dang, D.H., Schäfer, J., Brach-Papa, C., Lenoble, V., Durrieu, G., Dutruch, L., Chiffolleau, J.-F., Gonzalez,  
494 J.-L., Blanc, G., Mullot, J.-U., Mounier, S., Garnier, C., 2015b. Evidencing the Impact of Coastal  
495 Contaminated Sediments on Mussels Through Pb Stable Isotopes Composition. *Environ. Sci.*  
496 *Technol.* 49, 11438–11448. <https://doi.org/10.1021/acs.est.5b01893>
- 497 de Souza Machado, A.A., Spencer, K., Kloas, W., Toffolon, M., Zarfl, C., 2016. Metal fate and effects in  
498 estuaries: A review and conceptual model for better understanding of toxicity. *Science of The Total*  
499 *Environment* 541, 268–281. <https://doi.org/10.1016/j.scitotenv.2015.09.045>
- 500 Deborde, J., Anschutz, P., Auby, I., Glé, C., Commarieu, M.-V., Maurer, D., Lecroart, P., Abril, G., 2008.  
501 Role of tidal pumping on nutrient cycling in a temperate lagoon (Arcachon Bay, France). *Marine*  
502 *Chemistry* 109, 98–114. <https://doi.org/10.1016/j.marchem.2007.12.007>
- 503 Dong, S., Ochoa Gonzalez, R., Harrison, R.M., Green, D., North, R., Fowler, G., Weiss, D., 2017. Isotopic  
504 signatures suggest important contributions from recycled gasoline, road dust and non-exhaust  
505 traffic sources for copper, zinc and lead in PM 10 in London, United Kingdom. *Atmospheric*  
506 *Environment* 165, 88–98. <https://doi.org/10.1016/j.atmosenv.2017.06.020>
- 507 Dong, S., Wasylenki, L.E., 2016. Zinc isotope fractionation during adsorption to calcite at high and low  
508 ionic strength. *Chemical Geology* 447, 70–78. <https://doi.org/10.1016/j.chemgeo.2016.10.031>
- 509 Ducher, M., Blanchard, M., Balan, E., 2016. Equilibrium zinc isotope fractionation in Zn-bearing minerals  
510 from first-principles calculations. *Chemical Geology* 443, 87–96.  
511 <https://doi.org/10.1016/j.chemgeo.2016.09.016>
- 512 El Azzi, D., Viers, J., Guisresse, M., Probst, A., Aubert, D., Caparros, J., Charles, F., Guizien, K., Probst,  
513 J.L., 2013. Origin and fate of copper in a small Mediterranean vineyard catchment: New insights  
514 from combined chemical extraction and  $\delta^{65}\text{Cu}$  isotopic composition. *Science of The Total*  
515 *Environment* 463–464, 91–101. <https://doi.org/10.1016/j.scitotenv.2013.05.058>
- 516 Fauvelle, V., Belles, A., Budzinski, H., Mazzella, N., Plus, M., 2018. Simulated conservative tracer as a  
517 proxy for S-metolachlor concentration predictions compared to POCIS measurements in Arcachon  
518 Bay. *Marine Pollution Bulletin* 133, 423–427. <https://doi.org/10.1016/j.marpolbul.2018.06.005>

519 Fu, Z., Wu, F., Chen, L., Xu, B., Feng, C., Bai, Y., Liao, H., Sun, S., Giesy, J.P., Guo, W., 2016. Copper  
520 and zinc, but not other priority toxic metals, pose risks to native aquatic species in a large urban  
521 lake in Eastern China. *Environmental Pollution* 219, 1069–1076.  
522 <https://doi.org/10.1016/j.envpol.2016.09.007>

523 Gaetke, L.M., Chow-Johnson, H.S., Chow, C.K., 2014. Copper: Toxicological relevance and mechanisms.  
524 *Arch Toxicol* 88, 1929–1938. <https://doi.org/10.1007/s00204-014-1355-y>

525 Gamain, P., Cachot, J., Gonzalez, P., Budzinski, H., Gourves, P.-Y., Morin, B., 2017. Do Temporal and  
526 Spatial Parameters or Lifestyle of the Pacific Oyster *Crassostrea gigas* Affect Pollutant  
527 Bioaccumulation, Offspring Development, and Tolerance to Pollutants? *Frontiers in Marine*  
528 *Science* 4. <https://doi.org/10.3389/fmars.2017.00058>

529 Geffard, A., Amiard, J.C., Amiard-Triquet, C., 2002. Kinetics of metal elimination in oysters from a  
530 contaminated estuary. *Comparative Biochemistry and Physiology Part C: Toxicology &*  
531 *Pharmacology* 131, 281–293. [https://doi.org/10.1016/S1532-0456\(02\)00015-7](https://doi.org/10.1016/S1532-0456(02)00015-7)

532 Gonzalez, R., Weiss, D., 2015. Zinc Isotope Variability in Three Coal-Fired Power Plants: A Predictive  
533 Model for Determining Isotopic Fractionation during Combustion. *Environ. Sci. Technol.* 49,  
534 12560–12567. <https://doi.org/10.1021/acs.est.5b02402>

535 Guoinseau, D., Gélabert, A., Allard, T., Louvat, P., Moreira-Turcq, P., Benedetti, M.F., 2017. Zinc and  
536 copper behaviour at the soil-river interface: New insights by Zn and Cu isotopes in the organic-rich  
537 Rio Negro basin. *Geochimica et Cosmochimica Acta* 213, 178–197.  
538 <https://doi.org/10.1016/j.gca.2017.06.030>

539 Guoinseau, D., Gélabert, A., Moureau, J., Louvat, P., Benedetti, M.F., 2016. Zn Isotope Fractionation  
540 during Sorption onto Kaolinite. *Environ. Sci. Technol.* 50, 1844–1852.  
541 <https://doi.org/10.1021/acs.est.5b05347>

542 Hinard, G., 1932. Cuvrage accidentel et décuvrage de l’huitre. *Revue des Travaux de l’Institut des Pêches*  
543 *Maritimes* 331–365.

544 Křibek, B., Šípková, A., Ettler, V., Mihaljevič, M., Majer, V., Knésl, I., Mapani, B., Penížek, V., Vaněk,  
545 A., Sracek, O., 2018. Variability of the copper isotopic composition in soil and grass affected by  
546 mining and smelting in Tsumeb, Namibia. *Chemical Geology* 493, 121–135.  
547 <https://doi.org/10.1016/j.chemgeo.2018.05.035>

548 Krishnakumar, P.K., Qurban, M.A., Sasikumar, G., 2018. Biomonitoring of Trace Metals in the Coastal  
549 Waters Using Bivalve Molluscs, in: Saleh, H.E.-D.M., El-Adham, E. (Eds.), *Trace Elements -*  
550 *Human Health and Environment*. InTech. <https://doi.org/10.5772/intechopen.76938>

551 Kunene, S.C., Lin, K.-S., Mdlovu, N.V., Shih, W.-C., 2021. Bioaccumulation of trace metals and  
552 speciation of copper and zinc in Pacific oysters (*Crassostrea gigas*) using XANES/EXAFS  
553 spectroscopies. *Chemosphere* 265, 129067. <https://doi.org/10.1016/j.chemosphere.2020.129067>

554 Lawrence, D.R., Scott, G.I., 1982. The Determination and Use of Condition Index of Oysters. *Estuaries* 5,  
555 23. <https://doi.org/10.2307/1352213>

556 Le Berre, S., Courtel, J., Brigand, L., 2010. Etude de la fréquentation nautique du Bassin d’Arcachon.

557 Li, D., Liu, S.-A., Li, S., 2015. Copper isotope fractionation during adsorption onto kaolinite: Experimental  
558 approach and applications. *Chemical Geology* 396, 74–82.  
559 <https://doi.org/10.1016/j.chemgeo.2014.12.020>

560 Li, Wei, Gou, W., Li, Weiqiang, Zhang, T., Yu, B., Liu, Q., Shi, J., 2019. Environmental applications of  
561 metal stable isotopes: Silver, mercury and zinc. *Environmental Pollution* 252, 1344–1356.  
562 <https://doi.org/10.1016/j.envpol.2019.06.037>

563 Liu, S.-A., Huang, J., Liu, J., Wörner, G., Yang, W., Tang, Y.-J., Chen, Y., Tang, L., Zheng, J., Li, S.,  
564 2015. Copper isotopic composition of the silicate Earth. *Earth and Planetary Science Letters* 427,  
565 95–103. <https://doi.org/10.1016/j.epsl.2015.06.061>

566 Lu, D., Liu, Q., Zhang, T., Cai, Y., Yin, Y., Jiang, G., 2016. Stable silver isotope fractionation in the  
567 natural transformation process of silver nanoparticles. *Nature Nanotechnology* 11, 682–686.  
568 <https://doi.org/10.1038/nnano.2016.93>

569 Lu, G., Zhu, A., Fang, H., Dong, Y., Wang, W.-X., 2019. Establishing baseline trace metals in marine  
570 bivalves in China and worldwide: Meta-analysis and modeling approach. *Science of The Total*  
571 *Environment* 669, 746–753. <https://doi.org/10.1016/j.scitotenv.2019.03.164>

572 Lu, G.-Y., Ke, C.-H., Zhu, A., Wang, W.-X., 2017. Oyster-based national mapping of trace metals  
573 pollution in the Chinese coastal waters. *Environmental Pollution* 224, 658–669.  
574 <https://doi.org/10.1016/j.envpol.2017.02.049>

575 Lu, Y., Yuan, J., Lu, X., Su, C., Zhang, Y., Wang, C., Cao, X., Li, Q., Su, J., Ittekkot, V., Garbutt, R.A.,  
576 Bush, S., Fletcher, S., Wagey, T., Kachur, A., Sweijd, N., 2018. Major threats of pollution and  
577 climate change to global coastal ecosystems and enhanced management for sustainability.  
578 *Environmental Pollution* 239, 670–680. <https://doi.org/10.1016/j.envpol.2018.04.016>

- 579 Ma, L., Li, Y., Wang, W., Weng, N., Evans, R.D., Wang, W.-X., 2019. Zn Isotope Fractionation in the  
580 Oyster *Crassostrea hongkongensis* and Implications for Contaminant Source Tracking. *Environ.*  
581 *Sci. Technol.* 53, 6402–6409. <https://doi.org/10.1021/acs.est.8b06855>
- 582 Mai, H., Cachot, J., Brune, J., Geffard, O., Belles, A., Budzinski, H., Morin, B., 2012. Embryotoxic and  
583 genotoxic effects of heavy metals and pesticides on early life stages of Pacific oyster (*Crassostrea*  
584 *gigas*). *Marine Pollution Bulletin* 64, 2663–2670. <https://doi.org/10.1016/j.marpolbul.2012.10.009>
- 585 Martín, A., Caldelas, C., Weiss, D., Aranjuelo, I., Navarro, E., 2018. Assessment of Metal Immission in  
586 Urban Environments Using Elemental Concentrations and Zinc Isotope Signatures in Leaves of  
587 *Nerium oleander*. *Environ. Sci. Technol.* 52, 2071–2080. <https://doi.org/10.1021/acs.est.7b00617>
- 588 Mihaljevič, M., Baieta, R., Ettler, V., Vaněk, A., Kříbek, B., Penížek, V., Drahot, P., Trubač, J., Sracek,  
589 O., Chrástný, V., Mapani, B.S., 2019. Tracing the metal dynamics in semi-arid soils near mine  
590 tailings using stable Cu and Pb isotopes. *Chemical Geology* 515, 61–76.  
591 <https://doi.org/10.1016/j.chemgeo.2019.03.026>
- 592 Moynier, F., Vance, D., Fujii, T., Savage, P., 2017. The Isotope Geochemistry of Zinc and Copper.  
593 *Reviews in Mineralogy and Geochemistry* 82, 543–600. <https://doi.org/10.2138/rmg.2017.82.13>
- 594 Mulholland, D.S., Poitrasson, F., Boaventura, G.R., Allard, T., Vieira, L.C., Santos, R.V., Mancini, L.,  
595 Seyler, P., 2015. Insights into iron sources and pathways in the Amazon River provided by isotopic  
596 and spectroscopic studies. *Geochimica et Cosmochimica Acta* 150, 142–159.  
597 <https://doi.org/10.1016/j.gca.2014.12.004>
- 598 Ostrander, G.K. (Ed.), 1996. *Techniques in aquatic toxicology*. Lewis Publishers, Boca Raton, Fla.
- 599 Petit, J.C.J., Schäfer, J., Coynel, A., Blanc, G., Deycard, V.N., Derriennic, H., Lancelur, L., Dutruch, L.,  
600 Bossy, C., Mattielli, N., 2013. Anthropogenic sources and biogeochemical reactivity of particulate  
601 and dissolved Cu isotopes in the turbidity gradient of the Garonne River (France). *Chemical*  
602 *Geology* 359, 125–135. <https://doi.org/10.1016/j.chemgeo.2013.09.019>
- 603 Pourmozaffar, S., Tamadoni Jahromi, S., Rameshi, H., Sadeghi, A., Bagheri, T., Behzadi, S., Gozari, M.,  
604 Zahedi, M.R., Abrari Lazarjani, S., 2019. The role of salinity in physiological responses of  
605 bivalves. *Rev Aquacult raq*.12397. <https://doi.org/10.1111/raq.12397>
- 606 Rainbow, P.S., 2018. *Trace metals in the environment and living organisms: the British isles as a case*  
607 *study*. Cambridge University Press, Cambridge ; New York, NY.
- 608 Regoli, F., Orlando, E., 1994. Accumulation and subcellular distribution of metals (Cu, Fe, Mn, Pb and Zn)  
609 in the Mediterranean mussel *Mytilus galloprovincialis* during a field transplant experiment. *Marine*  
610 *Pollution Bulletin* 28, 592–600. [https://doi.org/10.1016/0025-326X\(94\)90360-3](https://doi.org/10.1016/0025-326X(94)90360-3)
- 611 Reilly, C., 2004. *The nutritional trace metals*. Blackwell Pub, Oxford, OX, UK ; Ames, IA, USA.
- 612 Resongles, E., Casiot, C., Freydier, R., Dezileau, L., Viers, J., Elbaz-Poulichet, F., 2014. Persisting impact  
613 of historical mining activity to metal (Pb, Zn, Cd, Tl, Hg) and metalloid (As, Sb) enrichment in  
614 sediments of the Gardon River, Southern France. *Science of The Total Environment* 481, 509–521.  
615 <https://doi.org/10.1016/j.scitotenv.2014.02.078>
- 616 Riget, F., Johansen, P., Asmund, G., 1997. Uptake and release of lead and zinc by blue mussels. Experience  
617 from transplantation experiments in Greenland. *Marine Pollution Bulletin* 34, 805–815.  
618 [https://doi.org/10.1016/S0025-326X\(97\)00028-3](https://doi.org/10.1016/S0025-326X(97)00028-3)
- 619 Rimmelin, P., Dumon, J.-C., Maneux, E., Gonçaves, A., 1998. Study of Annual and Seasonal Dissolved  
620 Inorganic Nitrogen Inputs into the Arcachon Lagoon, Atlantic Coast (France). *Estuarine, Coastal*  
621 *and Shelf Science* 47, 649–659. <https://doi.org/10.1006/ecss.1998.0384>
- 622 Roméo, M., Hoarau, P., Garello, G., Gnassia-Barelli, M., Girard, J.P., 2003. Mussel transplantation and  
623 biomarkers as useful tools for assessing water quality in the NW Mediterranean. *Environmental*  
624 *Pollution* 122, 369–378. [https://doi.org/10.1016/S0269-7491\(02\)00303-2](https://doi.org/10.1016/S0269-7491(02)00303-2)
- 625 Sauzéat, L., Costas-Rodríguez, M., Albalat, E., Mattielli, N., Vanhaecke, F., Balter, V., 2021. Inter-  
626 comparison of stable iron, copper and zinc isotopic compositions in six reference materials of  
627 biological origin. *Talanta* 221, 121576. <https://doi.org/10.1016/j.talanta.2020.121576>
- 628 Schleicher, N.J., Dong, S., Packman, H., Little, S.H., Ochoa Gonzalez, R., Najorka, J., Sun, Y., Weiss,  
629 D.J., 2020. A Global Assessment of Copper, Zinc, and Lead Isotopes in Mineral Dust Sources and  
630 Aerosols. *Front. Earth Sci.* 8. <https://doi.org/10.3389/feart.2020.00167>
- 631 Séguin, A., Caplat, C., Serpentine, A., Lebel, J.M., Menet-Nedelec, F., Costil, K., 2016. Metal  
632 bioaccumulation and physiological condition of the Pacific oyster (*Crassostrea gigas*) reared in two  
633 shellfish basins and a marina in Normandy (northwest France). *Marine Pollution Bulletin* 106,  
634 202–214. <https://doi.org/10.1016/j.marpolbul.2016.02.068>
- 635 Senez-Mello, T.M., Crapez, M.A.C., Ramos e Silva, C.A., Silva, E.T., Fonseca, E.M., 2020. Heavy metals  
636 bioconcentration in *Crassostrea rhizophorae*: A site-to-site transplant experiment at the Potengi  
637 estuary, Rio Grande do Norte, Brazil. *Sci Rep* 10, 246. <https://doi.org/10.1038/s41598-019-57152->  
638 w



- 639 Shiel, A.E., Weis, D., Cossa, D., Orians, K.J., 2013. Determining provenance of marine metal pollution in  
640 French bivalves using Cd, Zn and Pb isotopes. *Geochimica et Cosmochimica Acta* 121, 155–167.  
641 <https://doi.org/10.1016/j.gca.2013.07.005>
- 642 Shiel, A.E., Weis, D., Orians, K.J., 2012. Tracing cadmium, zinc and lead sources in bivalves from the  
643 coasts of western Canada and the USA using isotopes. *Geochimica et Cosmochimica Acta* 76,  
644 175–190. <https://doi.org/10.1016/j.gca.2011.10.005>
- 645 Shiel, A.E., Weis, D., Orians, K.J., 2010. Evaluation of zinc, cadmium and lead isotope fractionation  
646 during smelting and refining. *Science of The Total Environment* 408, 2357–2368.  
647 <https://doi.org/10.1016/j.scitotenv.2010.02.016>
- 648 Smith, K.E., Weis, D., Chauvel, C., Moulin, S., 2020. Honey maps the Pb fallout from the 2019 fire at  
649 Notre-Dame Cathedral, Paris: a geochemical perspective. *Environ. Sci. Technol. Lett.*  
650 <https://doi.org/10.1021/acs.estlett.0c00485>
- 651 Smith, K.E., Weis, D., Scott, S.R., Berg, C.J., Segal, Y., Claeys, P., 2021. Regional and global perspectives  
652 of honey as a record of lead in the environment. *Environmental Research* 195, 110800.  
653 <https://doi.org/10.1016/j.envres.2021.110800>
- 654 Souto-Oliveira, C.E., Babinski, M., Araújo, D.F., Weiss, D.J., Ruiz, I.R., 2019. Multi-isotope approach of  
655 Pb, Cu and Zn in urban aerosols and anthropogenic sources improves tracing of the atmospheric  
656 pollutant sources in megacities. *Atmospheric Environment* 198, 427–437.  
657 <https://doi.org/10.1016/j.atmosenv.2018.11.007>
- 658 Sullivan, K., Layton-Matthews, D., Leybourne, M., Kidder, J., Mester, Z., Yang, L., 2020. Copper Isotopic  
659 Analysis in Geological and Biological Reference Materials by MC-ICP-MS. *Geostand Geoanal  
660 Res* 44, 349–362. <https://doi.org/10.1111/ggr.12315>
- 661 Sun, R., 2019. Mercury Stable Isotope Fractionation During Coal Combustion in Coal-Fired Boilers:  
662 Reconciling Atmospheric Hg Isotope Observations with Hg Isotope Fractionation Theory. *Bull  
663 Environ Contam Toxicol* 102, 657–664. <https://doi.org/10.1007/s00128-018-2531-1>
- 664 Sussarellu, R., Lebreton, M., Rouxel, J., Akcha, F., Rivière, G., 2018. Copper induces expression and  
665 methylation changes of early development genes in *Crassostrea gigas* embryos. *Aquatic  
666 Toxicology* 196, 70–78. <https://doi.org/10.1016/j.aquatox.2018.01.001>
- 667 Tan, Q.-G., Wang, Y., Wang, W.-X., 2015. Speciation of Cu and Zn in Two Colored Oyster Species  
668 Determined by X-ray Absorption Spectroscopy. *Environ. Sci. Technol.* 49, 6919–6925.  
669 <https://doi.org/10.1021/es506330h>
- 670 Tonhá, M.S., Garnier, J., Araújo, D.F., Cunha, B.C.A., Machado, W., Dantas, E., Araújo, R., Kutter, V.T.,  
671 Bonnet, M.-P., Seyler, P., 2020. Behavior of metallurgical zinc contamination in coastal  
672 environments: A survey of Zn from electroplating wastes and partitioning in sediments. *Science of  
673 The Total Environment* 140610. <https://doi.org/10.1016/j.scitotenv.2020.140610>
- 674 Vance, D., Matthews, A., Keech, A., Archer, C., Hudson, G., Pett-Ridge, J., Chadwick, O.A., 2016. The  
675 behaviour of Cu and Zn isotopes during soil development: Controls on the dissolved load of rivers.  
676 *Chemical Geology* 445, 36–53. <https://doi.org/10.1016/j.chemgeo.2016.06.002>
- 677 Wallner-Kersanach, M., Theede, H., Eversberg, U., Lobo, S., 2000. Accumulation and Elimination of  
678 Trace Metals in a Transplantation Experiment with *Crassostrea rhizophorae*. *Arch. Environ.  
679 Contam. Toxicol.* 38, 40–45. <https://doi.org/10.1007/s002449910005>
- 680 Wang, W.-X., Meng, J., Weng, N., 2018. Trace metals in oysters: molecular and cellular mechanisms and  
681 ecotoxicological impacts. *Environ. Sci.: Processes Impacts* 20, 892–912.  
682 <https://doi.org/10.1039/C8EM00069G>
- 683 Wang, W.-X., Yang, Y., Guo, X., He, M., Guo, F., Ke, C., 2011. Copper and zinc contamination in oysters:  
684 Subcellular distribution and detoxification. *Environmental Toxicology and Chemistry* 30, 1767–  
685 1774. <https://doi.org/10.1002/etc.571>
- 686 Weiss, D.J., Rehkemper, M., Schoenberg, R., McLaughlin, M., Kirby, J., Campbell, P.G.C., Arnold, T.,  
687 Chapman, J., Peel, K., Gioia, and S., 2008. Application of Nontraditional Stable-Isotope Systems  
688 to the Study of Sources and Fate of Metals in the Environment. *Environ. Sci. Technol.* 42, 655–  
689 664. <https://doi.org/10.1021/es0870855>
- 690 Wijsman, J.W.M., Troost, K., Fang, J., Roncarati, A., 2019. Global Production of Marine Bivalves. Trends  
691 and Challenges, in: Smaal, A.C., Ferreira, J.G., Grant, J., Petersen, J.K., Strand, Ø. (Eds.), *Goods  
692 and Services of Marine Bivalves*. Springer International Publishing, Cham, pp. 7–26.  
693 [https://doi.org/10.1007/978-3-319-96776-9\\_2](https://doi.org/10.1007/978-3-319-96776-9_2)
- 694 Zalasiewicz, J.A. (Ed.), 2018. *The anthropocene as a geological time unit: a guide to the scientific evidence  
695 and current debate*. Cambridge University Press, Cambridge.
- 696 Zeng, J., Han, G., 2020. Preliminary copper isotope study on particulate matter in Zhujiang River,  
697 southwest China: Application for source identification. *Ecotoxicology and Environmental Safety*  
698 198, 110663. <https://doi.org/10.1016/j.ecoenv.2020.110663>

- 699 Zhong, Q., Yin, M., Zhang, Q., Beiyuan, J., Liu, J., Yang, X., Wang, J., Wang, L., Jiang, Y., Xiao, T.,  
700 Zhang, Z., 2021. Cadmium isotopic fractionation in lead-zinc smelting process and signatures in  
701 fluvial sediments. *Journal of Hazardous Materials* 411, 125015.  
702 <https://doi.org/10.1016/j.jhazmat.2020.125015>
- 703 Zhou, Q., Zhang, J., Fu, J., Shi, J., Jiang, G., 2008. Biomonitoring: An appealing tool for assessment of  
704 metal pollution in the aquatic ecosystem. *Analytica Chimica Acta* 606, 135–150.  
705 <https://doi.org/10.1016/j.aca.2007.11.018>  
706  
707

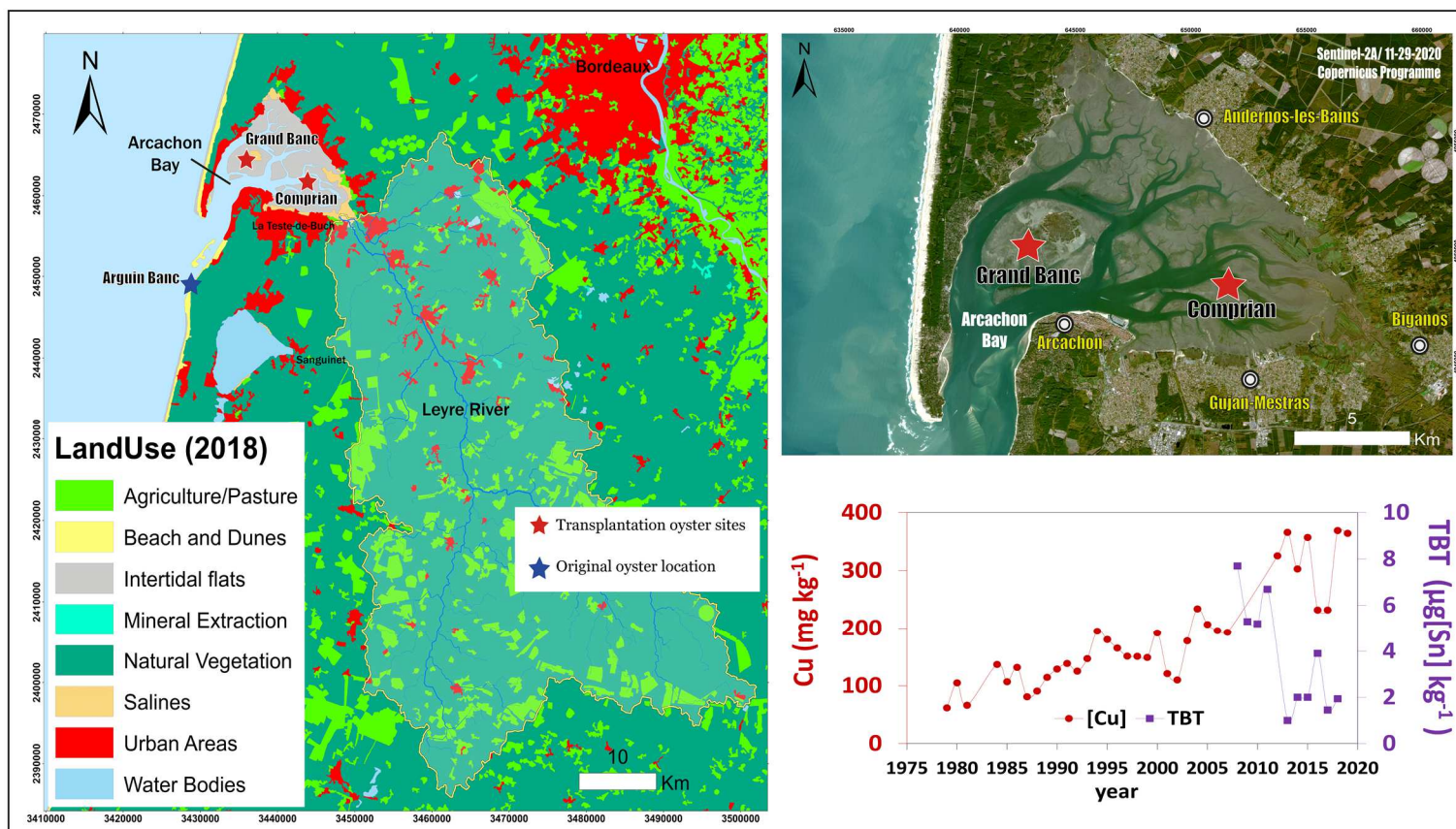


**Fig. 1.** Study site map and sampling stations. 18-month old oysters harvested from Arguin Banc were transplanted to Comprian and Grand Banc. The historical trends on Cu and TBT concentrations in indigenous oysters from the Comprian site are from ROCCH monitoring network (available at Surval: <https://wwz.ifremer.fr/surval/>).

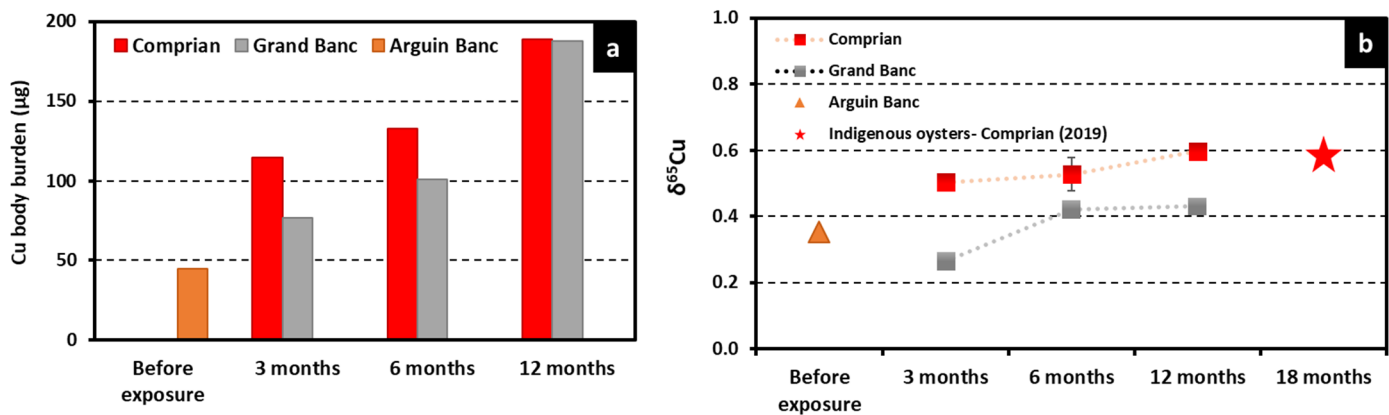


**Fig. 2.** (a) Temporal evolution of Cu body burden levels (Cu µg/per individual) and (b)  $\delta^{65}\text{Cu}$  values (‰) for oysters before (Arguin Banc) and after their transplantation in Arcachon Bay (AB), at Comprian and Grand Banc. The data refer to pools of oysters collected after three-, six-, and twelve-month long transplantation periods. An additional 2019 sample composed of 18-month old indigenous oysters was acquired from the French Mussel Watch program (ROCCH) environmental sample bank.

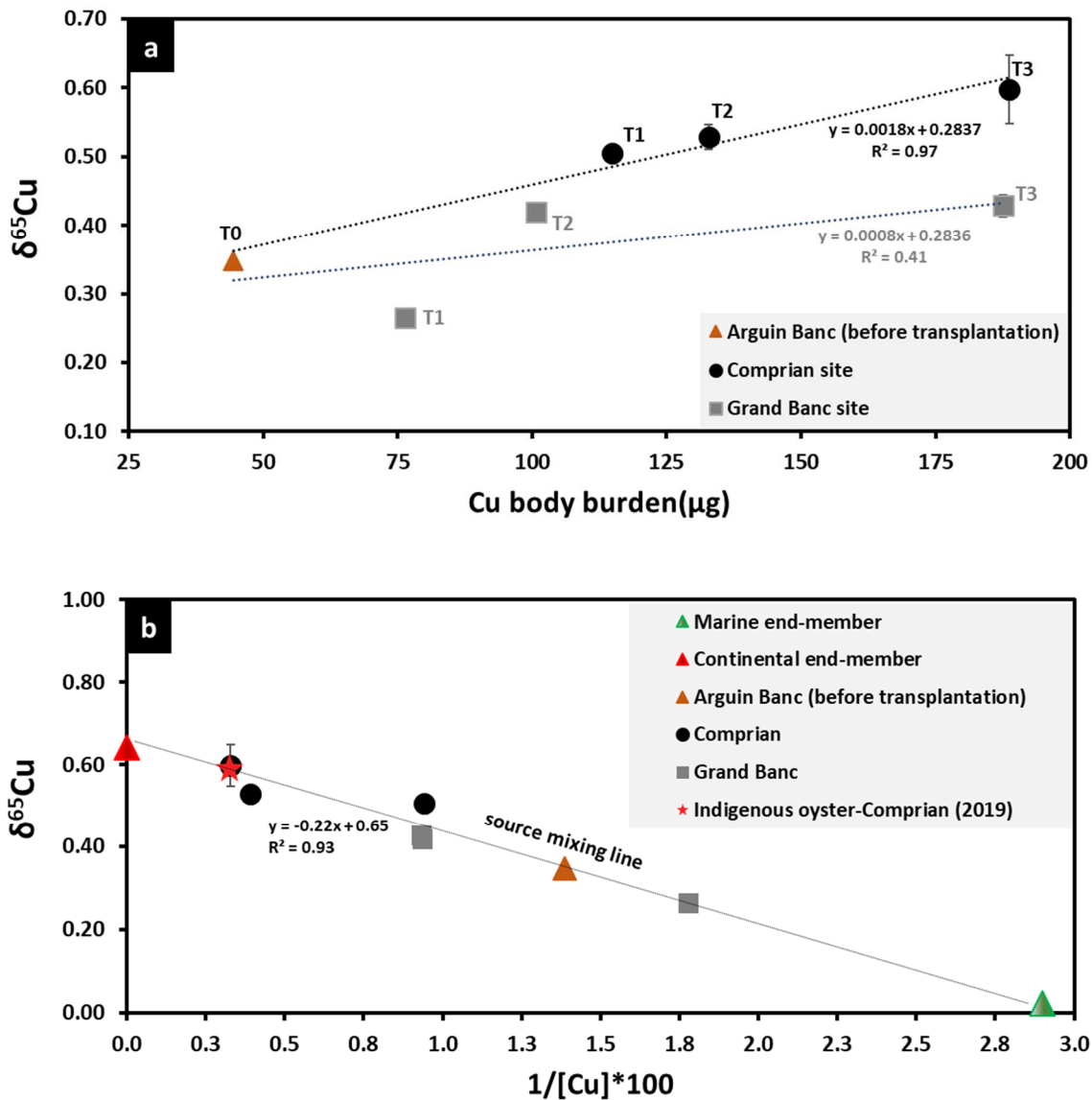


**Fig. 3.** (a) Plot of  $\delta^{65}\text{Cu}$  values (‰) against Cu body burden levels (Cu  $\mu\text{g}$ /individual bivalve) for oysters transplanted from Arguin Banc to the Comprian and Grand Banc sites; T1, T2, T3 labels refers to three-, six-, and twelve-month long transplantation periods. (b) Binary isotope source mixing model based on the regression analysis of oyster samples. The 2019 sample composed of indigenous oysters was acquired from the ROCCH sample bank. The natural bioaccumulated end-member is estimated at +0.02‰ using worldwide concentration baseline for oysters (Lu et al., 2019). The continental Cu end-member (+0.65‰) is estimated using the highest Cu concentration in the ROCCH database for Pacific oysters (2,5000  $\text{mg}\cdot\text{kg}^{-1}$ ). Error bars represent the analytical precision (2s) obtained for two measurements performed for each sample.

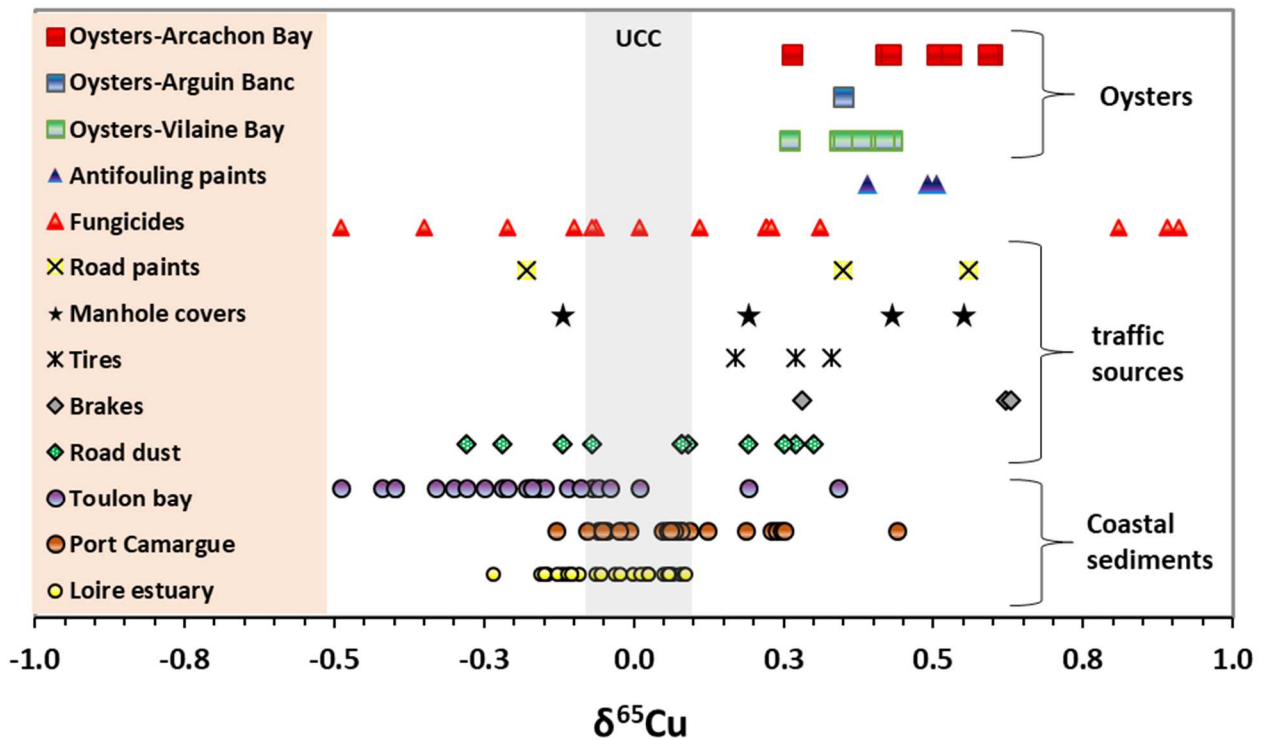


**Fig. 4.** Copper isotope compositions ( $\delta^{65}\text{Cu}$ , values in ‰) of oysters (this study) and anthropogenic materials reported in the literature: antifouling paints (Briant, 2014), fungicides (Babcsányi et al., 2016; Blotevogel et al., 2018; El Azzi et al., 2013), vehicle traffic-related sources (Dong et al., 2017; Schleicher et al., 2020; Souto-Oliveira et al., 2019). Oyster isotope data from Vilaine bay (Biscay Bay, Atlantic French shore) were published previously (Araújo et al., 2021a) and are included here for comparison. Coastal sediments include samples from Toulon bay (Araújo et al., 2019a), Port Camargue (French Mediterranean shore, Briant, 2014) and Loire estuary (Araújo et al., 2019c) (Biscay Bay, Atlantic French shore). They represent sediment isotope signatures related to harbor activities mixed to warfare contamination legacy, Cu-based antifouling paints and a low-Cu contaminated system, respectively. Grey band centered around 0 ‰ represents Cu isotope range average reported for Upper Continental Crust (UCC) (Liu et al., 2015).

**Table 1.** Copper concentrations, Cu body burden, and isotope compositions for dry-pooled oyster samples. The quantification of the continental Cu fraction (%) bioaccumulated in oysters using a binary isotope model is detailed in the text.

<b>Oyster sample ID</b>	<b>Exposure period</b>	<b>[Cu] (mg kg<sup>-1</sup>)</b>	<b>Cu body burden (µg)</b>	<b>δ<sup>65</sup>Cu (‰)</b>	<b>2s</b>	<b>Bioaccumulated continental Cu fraction (%)</b>
Oysters before exposure experiment (T0)	before exposure	72.1	44	0.35	0.06	52
Indigenous oyster (2019) in Comprian	18 months	305	ND	0.59	0.01	90
Transplanted oysters in Comprian						
Com-T1	3 months	106	115	0.50	0.01	77
Com-T2	6 months	257	133	0.53	0.02	81
Com-T3	12 months	304	189	0.60	0.05	92
Transplanted oysters in Grand Banc						
GB-T1	3 months	56	76	0.26	0.01	39
GB-T2	6 months	107	101	0.42	0.00	63
GB-T3	12 months	107	188	0.43	0.02	65

Graphical abstract

